Journal of Computer Assisted Tomography
24(3):416–420

Non-Hodgkin Lymphomas of the Ovaries: MR Findings

Francesco Ferrozzi, Giuseppe Tognini, Davide Bova, and Giulio Zuccoli

Purpose: The goal of this work was to describe MR findings (morphology, structure, signal intensity) of ovarian non-Hodgkin lymphoma (NHL).

Method: We reviewed the MR images of five female patients aged 13–70 years (mean 46 years) with histologically proven NHL of the ovaries. We evaluated morphological and signal intensity findings of the lesions. MR features were correlated with pathologic parameters.

Results: All the patients were affected by B-cell NHL; one patient showed a primary involvement of the ovaries; in one patient, ovarian disease was diagnosed 30 months after surgical resection of a primary uterine lymphoma; the remaining three had a systemic lymphoma. In three cases, the ovarian involvement was bilateral. The mean size of the lesions was 7.9 cm. All the lesions showed homogeneous low signal intensity on T1-weighted images and intermediate to high intensity on T2-weighted images. The postgadolinium images showed mild to moderate heterogeneous enhancement. The peripheral enhancement was better demonstrated in fat-suppressed images.

Conclusion: The diagnosis of primary ovarian lymphoma should be considered in the presence of large bilateral solid ovarian masses with homogeneous appearance (low signal on T1 and mildly high on T2) without infiltrative pattern of growth or regressive changes (necrosis, hemorrhage, calcifications) and with little contrast enhancement.

Index Terms: Ovary—Lymphoma—Magnetic resonance imaging.

The ovary is an exceedingly rare localization of lymphomas (1). In ~20% of the cases, non-Hodgkin lymphoma (NHL) presents as extranodal disease, <1% beginning primarily in the ovary (2,3). Ovarian lymphomas are generally considered the local manifestation of an occult lymphonodal disease or a secondary site of a systemic disease (2). Symptoms are rarely present and are for the most nonspecific (3). The clinical picture of a B-cell lymphoma is only occasionally seen (1). Therefore, the detection of ovarian lymphoma is often incidental, and its differentiation from other solid ovarian masses and from pedunculated intraligamentous uterine leiomyomas has important clinical and therapeutic implications.

MRI, thanks in particular to rapid technological progress, has become the imaging procedure of choice for "in vivo" characterization of adnexal lesions (4–7). In this article, we present MR findings in five cases of pathologically proven malignant lymphomas of the ovaries.

From the Istituto di Scienze Radiologiche, Università degli Studi di Parma, Parma, Italy. The current address of Dr. D. Bova is Department of Radiology, Loyola University Medical Center, Maywood, IL, U.S.A. Address correspondence and reprint requests to Dr. F. Ferrozzi at Istituto di Scienze Radiologiche, Università degli Studi di Parma, Via Gramsci 14, 43100 Parma, Italy. E-mail: fferrozzi@netsis.it

MATERIALS AND METHODS

Among all the MR and pathologic records of extranodal lymphomas between January 1993 and December 1998, we retrospectively selected five female patients who underwent MRI of the pelvis. Their age ranged from 13 to 70 years (mean 46 years). The diagnosis of NHL was pathologically confirmed in one case by needle core biopsy, in two cases at surgery, and in the remaining two by autopsy.

All our cases were B-cell NHL, diffuse type in four cases and follicular in the remaining one. In one of our patients, the lesions were considered as primary lymphoma of the ovary, whereas all the others had a secondary involvement of the ovaries. Secondary lymphomas were diagnosed at the time of clinical presentation of disease in two cases or at the time of disease relapse in two cases.

In four cases, MRI was performed with a 1.5 T unit (Vision; Siemens Medical Systems, Erlangen, Germany) and in one case with a 0.5 T unit (T5 II; Philips Medical Systems, Eindhoven, the Netherlands). Multiplanar (axial, coronal, sagittal) conventional T1- and T2-weighted spin echo images were acquired. Additional T1-weighted fat saturation images after administration of Gd-DTPA were also obtained in three patients.

Morphologic features such as tumor location, size, morphology, contours, invasion of neighboring structures, lymphadenopathies, and signal intensity characteristics were analyzed. Lesions were described as homogeneous or heterogeneous. Signal intensity was rated as low, intermediate, or high relative to the signal intensity of the muscle in sequences both with and without Gd.

RESULTS

Among the five patients, three had bilateral lesions (Figs. 1 and 2) and the other two unilateral (Fig. 3) (right ovary in one and left in one), for a total of eight lesions. The lesions ranged in diameter from 4 to 10 cm (mean 7.9 cm).

The histologic types were Burkitt lymphoma in one, diffuse immunoblastic large B-cell in two, follicular large B-cell in one, and diffuse lymphoplasmocytic B-cell in one. In all but one patient, concurrent lesions were detected in bone marrow, peritoneum, liver, spleen, kidney, adrenal glands, and thoracic, abdominal, and pelvic lymph nodes.

In the case of primary lymphoma, the clinical presentation was characterized by diffuse arthralgia, back pain, and systemic symptoms. In four patients, a palpable mass in the pelvis was found at physical examination. Two patients presented with fever and three with pain (Table 1).

Survival ranged from 8 to 20 months from the time of detection of ovarian disease (mean 14 months). Two patients are still alive, one with diffuse lymphomatous multisystemic involvement and one free of disease. In one patient, ovarian disease was diagnosed 30 months after surgical resection of a primary uterine lymphoma.

All the lesions had well defined margins and were primarily round or oval in morphology. Contours were lobulated in three and smooth in two. The lesions exhibited homogeneously low signal intensity on T1-weighted images (Figs. 1A–3A), intermediate to high intensity on T2-weighted images (Fig. 2B), and mild to moderate heterogeneous contrast enhancement after intravenous administration of Gd-DTPA (Figs. 1C and 2C). Three patients showed predominantly peripheral contrast enhancement in fat-suppressed post-Gd T1-weighted sequences (Fig. 3D).

DISCUSSION

NHL presents as extranodal disease in 20% of cases. Ovary involvement in primary parenchymal localizations is exceedingly rare (2). The origin of primary ovarian lymphoma seems to be independent of the presence of normal lymphoid tissue in the ovary (3).

A lymphomatous mass of the ovary may represent the first manifestation of an occult nodal disease or a secondary localization due to systemic diffusion of disease (3). Although several authors have proposed different diagnostic criteria for primary ovarian lymphoma, no real consensus exists on the topic. According to the more or less restrictive criteria adopted for diagnosis, the incidence of true primary lymphoma of the ovary ranges from 2% (8) to 18% (9) of suspected cases. This is why several authors (3,8) regard as more prudent the consideration of ovarian lymphoma as the local manifestation, albeit solitary, of a disease that has already reached systemic proportions.

The clinical appearance of ovarian lymphoma is nonspecific. Symptoms of an abdominal-pelvic mass (67%) (3) with or without pain, vaginal bleeding, amenorrhea, irregular menses, osteoarticular aches, and ascites are the most common findings. B-Lymphomatous symptoms are only occasionally reported (17%) (3). On rare occasions, the tumor is entirely asymptomatic and its detection absolutely incidental. Laboratory data, biohumoral parameters, and hormonal levels are often nondiagnostic (10).

Ninety-six percent of primary lymphomas of the ovary are of B-lymphocyte origin, according to the literature (11), and the great majority of them is of diffuse type. Among pediatric NHL, the noncleaved small cell type, either Burkitt (Fig. 1) or non-Burkitt, is the most com-

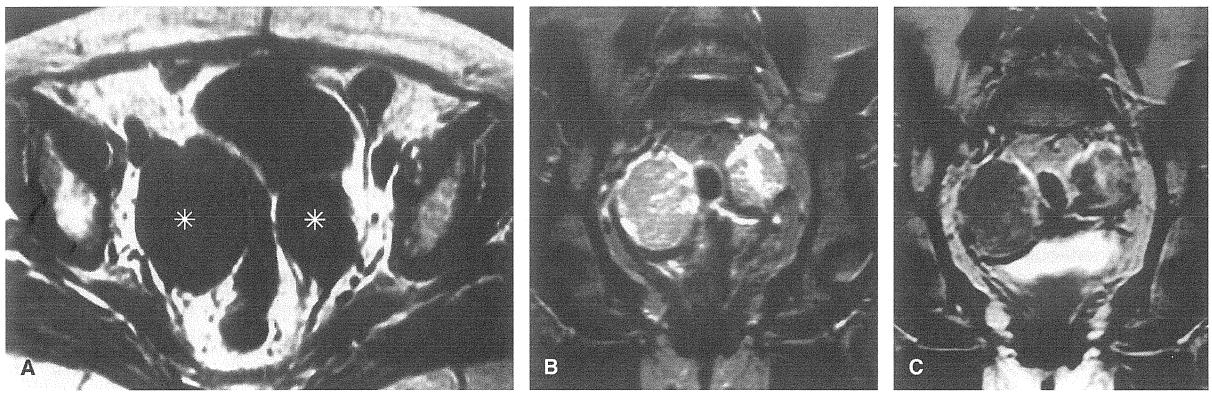

FIG. 1. A 42-year-old woman with pelvic mass, abdominal pain, and lymphedema of the legs. **A:** Axial T1-weighted image demonstrates bilateral oval well defined masses in the adnexal region, with homogeneously hypointense appearance. The right mass abuts the sigmoid wall. **B and C:** T2-weighted coronal image (B) shows the heterogeneous high signal intensity of the masses, which demonstrates mild irregular contrast enhancement in the postgadolinium image (C). Fine needle biopsy demonstrates Burkitt non-Hodgkin lymphoma.

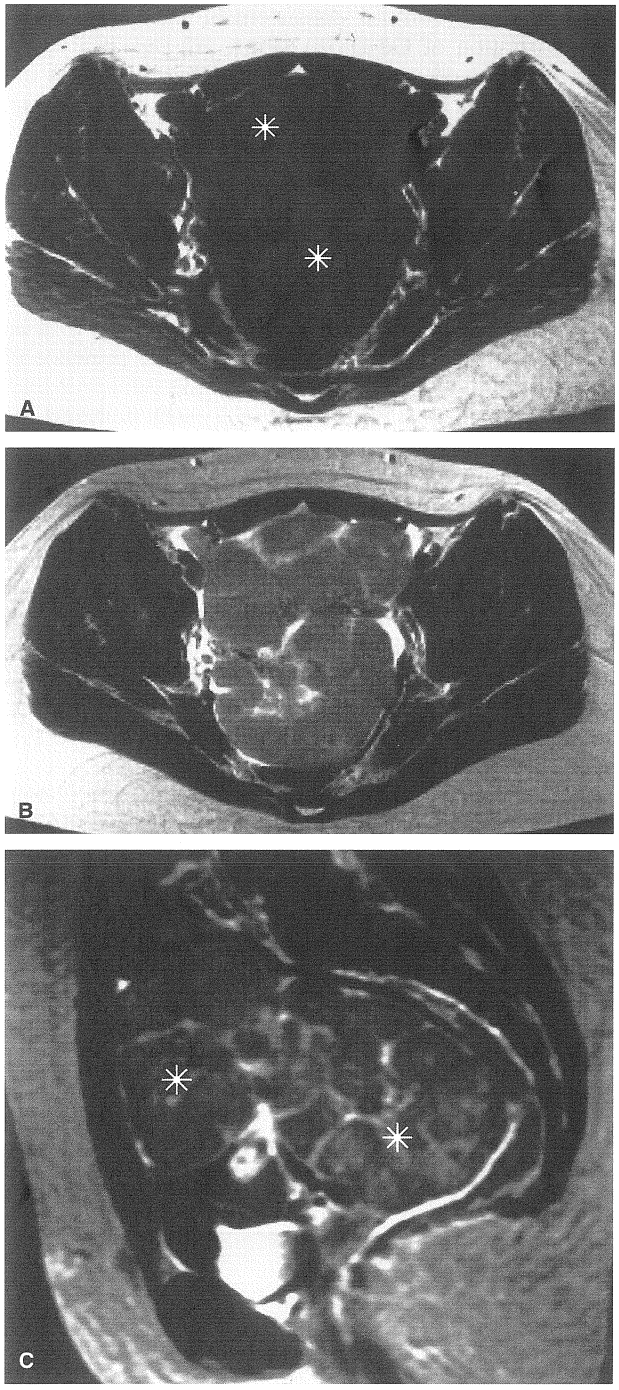

FIG. 2. A 13-year-old girl with fever, back pain, and arthralgia. **A and B:** Axial T1-weighted (A) and T2-weighted (B) images of the pelvis show bilateral large lobulated masses, with smooth borders and homogeneous signal. **C:** Sagittal postgadolinium image shows intermediate and irregular enhancement of the masses with "cerebroid" appearance. Pathologic specimen demonstrates bilateral non-Hodgkin lymphoma of the ovary, B-cell, diffuse "lymphoplasmocytoid type."

mon subtype in this organ, accounting for 38% of cases (3). The next most frequent subtype is diffuse large cell lymphoma (Figs. 2 and 3), whereas follicular lymphomas are very rare and Hodgkin lymphomas have never been described in the ovary (1,2,9,10). Their prognosis is variable and depends on several factors (12). Advanced stage, bilaterality of lesions, the non-B-lymphocyte origin, the presence of systemic symptoms, and an acute onset are associated with a poor prognosis (9,10,12). Surgery followed by adjuvant chemotherapy is the most efficacious treatment protocol (3,10,12).

No specific radiologic or imaging features have been found to offer specific indications of an ovarian lymphoma. From the diagnostic point of view, ultrasonography, in spite of its sensitivity in detecting abdominal and pelvic lymphomatous masses, does not offer reliable criteria for characterization of ovarian lymphomas. The homogeneously hypoechoic appearance and the lack of significant vascularity on color Doppler mapping constitute the most frequently encountered appearance of these lesions (13).

The CT structural features that may lead to diagnosis of lymphoma have already been described at length (14). The relative structural homogeneity (Fig. 1), without significant necrosis, hemorrhage, or calcifications, the relative hypovascularity, and frequent bilaterality or multicentricity are all more frequently seen in lymphomatous masses than in solid malignancies and are valid in the ovary as well.

MRI offers analogous structural depiction of lesions and of their vascularization. In addition, it is accurate in assessing the topography and spatial relations of pelvic masses thanks to its multiplanar capabilities and the lack of respiratory or peristaltic motion artifacts (6). In particular, coronal and sagittal images (Figs. 1 and 2) are particularly useful in evaluating the organ of origin when the pelvic mass is voluminous and extends beyond the anatomical borders of the pelvis itself.

At MRI, ovarian lymphomas present as solid bilateral masses. The signal characteristics of ovarian lymphoma are the same as seen in lymphomatous lesions in other locations, with hypointensity on T1-weighted images and homogeneous and mild hyperintensity on T2-weighted images. Contrast enhancement after intravenous administration of gadolinium is mild to moderate, and fat-suppressed T1-weighted images demonstrate the enhancement to better advantage; in fact, in our patients, the peripheral contrast enhancement seems to be typical.

Bilateral ovarian lymphomas should be differentiated from metastatic involvement of the ovaries. Ovarian metastases represent ~30% of all ovarian neoplasms and are sometimes diagnosed before the primary tumor (15). In decreasing order of frequency, the primary tumors are colon, stomach, breast, pancreas, gallbladder, and bronchogenic carcinomas, as well as melanoma. Ovarian metastases are generally bilateral with mixed appearance (solid and cystic); metastases with high fibrous component (particularly from gastrointestinal tract) often show hypointense areas on T2-weighted images with strong contrast enhancement (15).

The rare primary forms must be differentiated from ovarian neoplasms with a stromal or mesenchymal component, such as the fibroma, fibrothecoma (16), teratoma

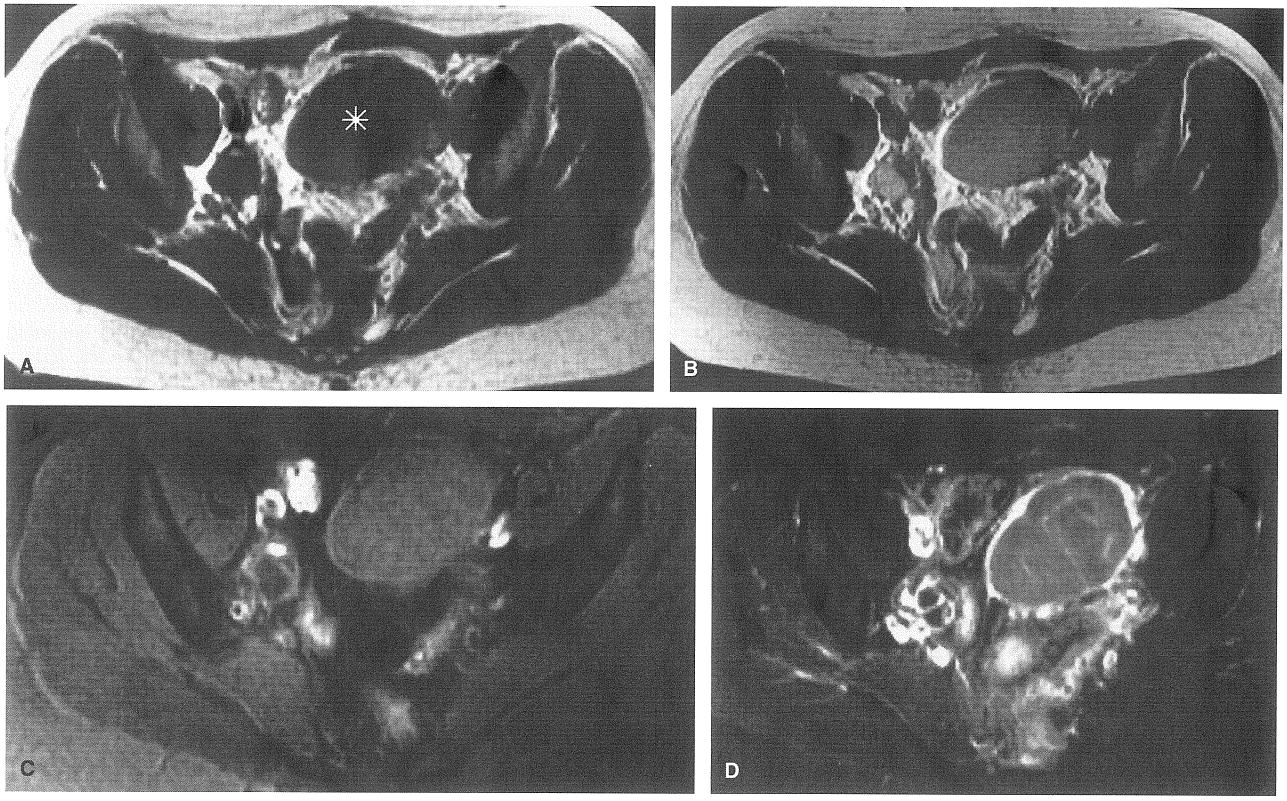

FIG. 3. A 40-year-old woman with pelvic mass, who underwent surgical resection 30 months before for primary immunoblastic lymphoma of the uterus. **A:** Axial short TR short TE image of the pelvis shows a large oval lesion, homogeneously hypointense and with smooth borders originating from the left adnexal region. **B:** The lesion appears mildly hyperintense, without necrotic component on proton density sequence. **C and D:** Fat-suppressed short TR short TE sequence demonstrates the homogeneous appearance of the lesion (C), which shows low homogeneous enhancement of the mass with a peripheral rim of marked enhancement (D). Surgical resection confirmed the ovarian relapse.

(17,18), or neoplasms containing ectopic tissue as struma ovarii (19). In tumors with a fibrous component, the consistent hypointensity on T2-weighted images generally allows a rather easy diagnosis (16), and the typical signals of fat are reliably associated with teratomatous lipid components (18,19).

The solid epithelial neoplasms, especially if not yet associated with ascites (which is rare even in advanced peritoneal lymphomatous lesions) and peritoneal carcinomatosis, may, on the other hand, be differentiated from lymphomas if they present a complex structure due to cystic loculations, more frequent necrosis and hemorrhage, and more pronounced and yet more heterogeneous contrast enhancement (5).

Very large masses of the pelvis include sarcomas originating from pelvic mesenchymal tissues and, in the pediatric age group, neuroblastoma (4). Again, the relatively homogeneous structure and little contrast enhance-

TABLE 1. *Summary of cases of ovarian lymphoma*

Age (yrs)	Histology	Location	Size (cm)	Synchronous locations	Symptoms	Survival
13	Diffuse lymphoplasmocytic B-cell NHL	Bilateral	Rt = 9 × 6, Lt = 9 × 7	Bone marrow, pelvic peritoneum	Arthralgia, fever, back pain	14 mos alive, disease-free
70	Diffuse immunoblastic large B-cell NHL	Bilateral	Rt = 5 × 6, Lt = 10 × 6	Liver, spleen, kidney abdominal-pelvic lymph nodes	Pelvic mass, abdominal pain	14 mos
42	Burkitt B-cell NHL	Bilateral	Rt = 10 × 9, Lt = 8 × 7	Bone marrow, pelvic peritoneum, pelvic lymph nodes	Lymphedema of legs, abdominal pain, pelvic mass	8 mos
64	Follicular large B-cell NHL	Right ovary	Rt = 5 × 4	Pelvic lymph nodes, liver, spleen	Fever, pelvic mass	20 mos
40	Diffuse immunoblastic large B-cell NHL	Left ovary	Lt = 5 × 6	None	Pelvic mass	5 mos alive, diffuse disease

NHL, non-Hodgkin lymphoma.

ment are suggestive of a lymphomatous mass, whereas sarcomas more often exhibit an early tendency to extensive necrosis and are hypervascular. The macrocalcifications often demonstrated in neuroblastomas may also be discriminating as foci without signal.

The much more frequent clinical scenario of plurivisceral involvement by lymphoma and its associated generalized lymphadenopathy, with the above-described signal characteristics, are, however, highly suggestive of the correct diagnosis.

CONCLUSION

Despite its rarity and its lack of pathognomonic imaging features, the diagnosis of "primary" ovarian lymphoma must be considered when in the presence of large bilateral ovarian masses, with lobulated and homogeneous appearance (low signal on T1, mildly high on T2) and without macroscopic signs of infiltration, significant necrosis, or marked contrast enhancement. The association of these features with multiple lesions in other locations and organs, either at staging or follow-up of lymphomas, does not, on the other hand, pose significant diagnostic difficulties.

Acknowledgment: The authors are grateful to Dr. Naomi Wangui Mulonzia for revising the manuscript.

REFERENCES

1. Osborne BM, Robboy SJ. Lymphoma or leukemias as ovarian tumors: an analysis of 42 cases. *Cancer* 1983;52:1933–43.
2. Chorlton I, Norris HJ, King FM. Malignant reticuloendothelial disease involving the ovary as a primary manifestation: a series of 19 lymphomas and 1 granulocytic sarcoma. *Cancer* 1974;34:397–407.
3. Monterosso V, Jaffe ES, Merino MJ, et al. Malignant lymphomas involving the ovary: a clinicopathologic analysis of 39 cases. *Am J Surg Pathol* 1993;17:154–70.
4. Hugosson C, Nyman R, Jacobsson B, et al. Imaging and compartmental classification of solid pelvic tumours in children. *Pediatr Radiol* 1996;26:861–8.
5. Scoutt LM, McCarthy SM, Lange R, et al. MR evaluation of clinically suspected adnexal masses. *J Comput Assist Tomogr* 1994;18:609–19.
6. Reuter M, Steffens JC, Schupper U, et al. Critical evaluation of the specificity of MRI and TVUS for differentiation of malignant from benign adnexal lesions. *Eur Radiol* 1998;8:39–44.
7. Shapiro I, Lanir A, Sharf M, et al. Magnetic resonance imaging of gynecologic masses. *Gynecol Oncol* 1987;28:186–91.
8. Nelson GA, Dockerty MB, Pratt JH, et al. Malignant lymphoma involving the ovaries. *Am J Obstet Gynecol* 1958;76:861–71.
9. Paladugu RR, Bearman RM, Rappaport H. Malignant lymphoma with primary manifestation in the gonad: a clinicopathologic study of 38 patients. *Cancer* 1980;45:561–71.
10. Fox H, Langley FA, Govan ADT, et al. Malignant lymphoma presenting as an ovarian tumor: a clinicopathologic analysis of 34 cases. *Br J Obstet Gynecol* 1988;95:386–90.
11. Skodras G, Fields V, Kragel PJ. Ovarian lymphoma and serous carcinoma of low malignant potential arising in the same ovary: a case report with literature review of 14 primary ovarian lymphomas. *Arch Pathol Lab Med* 1993;118:647–52.
12. Freeman C, Berg JW, Cutler SJ. Occurrence and prognosis of extranodal lymphoma. *Cancer* 1972;29:252–60.
13. Gorg C, Weide R, Schwerk WB. Sonographic patterns in extranodal abdominal lymphomas. *Eur Radiol* 1996;6:855–64.
14. Ferrozzi F, Campani R, Garlaschi G, et al. Extranodal lymphomas: CT findings and differential diagnosis. *Radiol Med* 1997;93:429–441.
15. Kim SH, Kim WH, Park KJ, et al. CT and MR findings of Krukenberg tumors: comparison with primary ovarian tumors. *J Comput Assist Tomogr* 1996;20:393–8.
16. Troiano RN, Lazzarini KM, Scoutt LM, et al. Fibroma and fibrothecoma of the ovary: MR imaging findings. *Radiology* 1997;204:795–8.
17. Tanaka YO, Kurosaki Y, Nishida M, et al. Ovarian dysgerminoma MR and CT appearance. *J Comput Assist Tomogr* 1994;18:443–7.
18. Togashi K, Nishimura K, Itoh K, et al. Ovarian cystic teratomas: MR imaging. *Radiology* 1991;180:73–8.
19. Dohke M, Watanabe Y, Takahashi A, et al. Struma ovarii: MR findings. *J Comput Assist Tomogr* 1997;21:265–7.